Optimum Excitations for a Dual-Band Microwatt Wake-Up Radio

Massimo Del Prete, *Student Member, IEEE*, Alessandra Costanzo, *Senior Member, IEEE*, Michele Magno, *Senior Member, IEEE*, Diego Masotti, *Member, IEEE*, and Luca Benini, *Fellow, IEEE*

***Abstract*— To enable pervasive exploitation of wireless sensor networks, semipassive wake-up radios (WuRs) are proposed to minimize the active time of the energy-hungry main communication radio. The most challenging feature is to enhance their sensitivity, the weakest activation signal the receiver is able to sense, which is limited by the minimum turn-on voltage of the diode-based detector. In order to operate the detector at even lower power levels, a strategy to optimize the modulated WuR excitations is presented, exploiting high-peak intermittent continuous waves while preserving the required average power per bit. The design and implementation of an ultralow-power detector, fed by a dual-band antenna and loaded by the WuR backend is presented: 2.45-GHz and 868-MHz operations of the same WuR are demonstrated, with added flexibility and interoperability among different communication bands. We show that a correct WuR activation is possible with an average power per bit as low as −63 dBm at 2.45 GHz and −65 dBm at 868 MHz. This is experimentally verified by a lab-level setup and confirmed by a system implementation based on off-the-shelf components only.**

***Index Terms*— Power optimized waveforms (POWs), RF rectifier, ultralow power wake-up radio (WuR).**

I. Introduction

THE requirements of ultralow power Internet-of-things-like applications have recently focused the research interests in lowering the power needs of wireless sensor networks (WSNs). The most energy-hungry part of such nodes is the radio transceiver due to its power consumption in the idle mode of operation. To enhance communication efficiency, the main radio transceiver should be kept in sleep mode, most of the time, and be activated only when the related node is effectively interrogated. Among the proposed energy-aware solutions, asynchronous-type transceivers with passive wake-up radio (WuR) solutions seem to be extremely promising. Such RF systems have the role of continuously listening to the transmission medium and of waking up the main radio, upon detection of the incoming message. Highly efficient WuRs, able to operate with power consumption of the order of a few microwatts, or even hundreds of nanowatts, have been experimentally demonstrated [1], [2]. However, limited energy availability still remains the crucial issue. Hence, effective adoption of WuR-based nodes relies on the fulfillment of two different requirements at the same time: 1) minimization of power consumption for listening the channel: this should be orders of magnitude lower than that of the main radio and 2) enhancement of WuR sensitivity, which can be defined as the weakest activation signal the WuR is able to detect, and is directly related to the maximum communication distance.

A possible WuR implementation is shown in Fig. 1(a), where the circuit schematics of the RF and baseband subsystems of a WuR are shown. A dual-band antenna, designed to operate at 868 and 2450 MHz, the envelope detector, and their matching network compose the WuR RF frontend to convert the RF signal into baseband (V_{dc}); such a signal is the input of an ultralow power comparator that needs to extract the information and generate the interrupt signals and data to the on-board ultralow power microcontroller. Fig. 1(b) shows a first prototype of the wake-up system architecture. In order to enhance the detector sensitivity, its excitations should be precisely shaped accounting for the average ultralow powers to be targeted (lower than −40 dBm).

Power optimized waveforms (POWs) have been successfully presented in the past few years to improve the system performance in different applications: in [3] and [4], they allow to enlarge RFIDs' reading range, whereas in [5] and [6], higher rectenna efficiencies are achieved in energy harvesting (EH) and wireless power transfer scenarios. In [6], closed-form equations, theoretically justifying the convenience in utilizing high peak-to-average power ratio (PAPR) waveform, are provided and fairly good agreement with experimental data is observed. However, it is proved that such kinds of waveforms improve the system performance in precise RF power ranges that are much higher than those of interest for the WuR [3].

In [7], a preliminary experimental analysis has been carried out at 868 MHz only, and it has been proved that WuR sensitivity can be pushed down to −65 dBm by exploiting intermittent continuous wave (ICW) with high peaks in short-time instants [8], while maintaining the same average power in a bit interval. This paper expands upon [7] and provides a theoretical validation of the results by analytically computing the detector behavior at such extremely low excitation levels.

Manuscript received July 1, 2016; revised September 20, 2016; accepted October 23, 2016. Date of publication November 17, 2016; date of current version December 7, 2016. This work was supported by EU COST Action IC1301 "Wireless Power Transmission for Sustainable Electronics" (WIPE). This work was supported in part by the Italian Ministry of the Instruction, University and Research (MIUR), within the framework of the national project GRETA. An earlier version of this paper was presented at the IEEE MTT-S International Microwave Symposium, San Francisco, CA, USA, May 22–27, 2016.

M. Del Prete, A. Costanzo, and D. Masotti are with the Department of Electrical, Electronic and Information Engineering, "Guglielmo Marconi," University of Bologna, 40126 Bologna, Italy (e-mail: massimo.delprete3@unibo.it; alessandra.costanzo@unibo.it; diego.masotti@unibo.it).

M. Magno and L. Benini are with the Department of Information Technology and Electrical Engineering, ETH Zürich, 8092 Zürich, Switzerland (e-mail: mmagno@iis.ee.ethz.ch; lbenini@iis.ee.ethz.ch).

Color versions of one or more of the figures in this paper are available online at http://ieeexplore.ieee.org.

Digital Object Identifier 10.1109/TMTT.2016.2622699

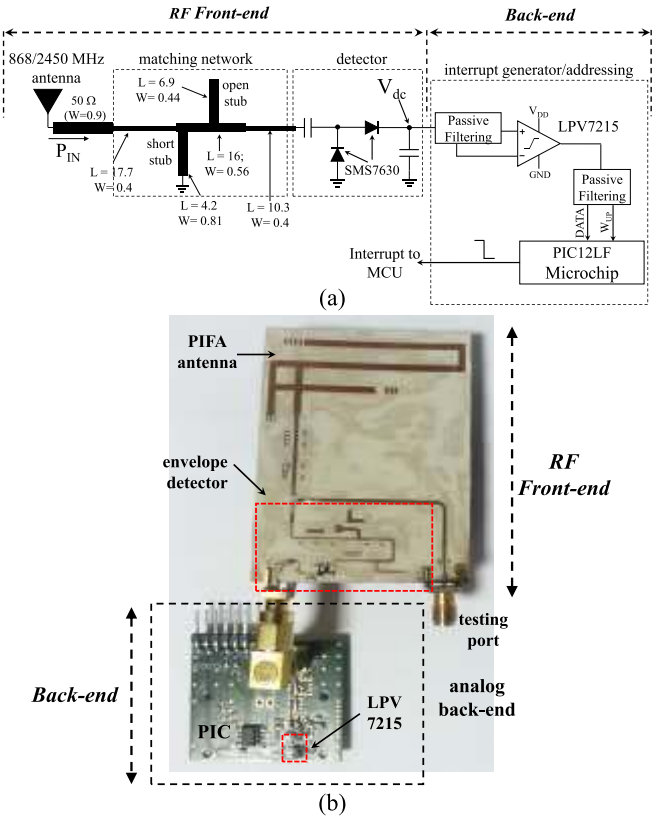

Fig. 1. (a) Schematic of the asynchronous-type WuR and sizes of the designed matching network in mm. (b) Implemented WuR system [7].

From the nonlinear relationship between the detector output voltage and its excitations, a figure of merit, which is the ratio between the dc-voltage envelopes, obtained with the optimized waveforms and with the CW excitations, is analytically computed and used to evaluate the different possible optimized waveforms. Depending on the diode operating regions, it is demonstrated that selected ICWs can be adopted while multisine excitations do not provide any advantages over their CW counterparts. This is then validated over the two bands of interest, by means of nonlinear simulations and by measurements over the two frequencies' band of operations. The proposed new strategy demonstrates that, with the reduction of the waveform duty cycle, higher power peaks can be exploited, still maintaining the same average RF power per bit interval: average RF power per bit as low as -65 dBm becomes sufficient for WuR operation with ICW. Finally, an experimental validation is also presented and it is shown that such WuR exciting conditions can be obtained making use of off-the-shelf components.

II. Overview of the Dual-Band Wake-up Radio

Here we briefly describe and experimentally validate the dual-band RF unit of the WuR, shown in Fig. 1(b), whose simulated behavior only was presented in [9]. A PIFA-like, dual-band, low-profile antenna is adopted to simultaneously operate in the 868- and 2450-MHz bands. Its layout is again shown in Fig. 1(b) and is based on a 635-μm-thick RF-60A-Taconic substrate ($\varepsilon_r = 6.15$, $\tan\delta = 0.0038$ at 10 GHz). The antenna is a combination of two monopoles,

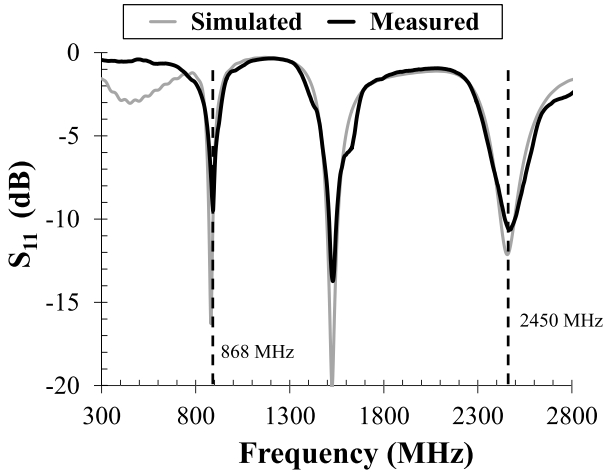

Fig. 2. Simulated and measured antenna reflection coefficient versus frequency.

whose lengths are optimized to tune the antenna at the required resonant frequencies with the highest radiation efficiency and a monopole-like radiation pattern at the two operating frequencies. The measured and simulated performances of the antenna, in terms of input reflection coefficient, are shown in Fig. 2: very good agreement has been obtained with the full-wave simulation (CST Microwave Studio 2013). An additional resonance is obtained at about 1.5 GHz due to the combined effect of the two branches, which does not affect the present design. It is noteworthy that this RF section of the WuR is designed in such a way as to present end-to-end continuity between the antenna and the detector, thus allowing to minimize the matching network elements with the twofold advantage of reducing the overall node size and losses. The latter are small in absolute, although significant for the purposes of our work, given the ultralow power involved. The detector is a single-stage full-wave Dickson voltage doubler rectifier. The diodes are selected based on their sensitivity, defined as the highest dc voltage at a given (low) input RF power. The SMS7630-079 (Skyworks Inc.) results to be the best compromise among sensitivity, losses, and operating frequencies to be covered. Another challenging task of the detector design is the multiband matching network that requires to account for the dispersive and nonlinear behavior of the overall system affecting the power-dependent detector input impedance [10].

The chosen topology is shown in Fig. 1(b) and consists of two impedance steps and two stubs, the first shorted and the second open. Impedance steps are employed to guarantee a wideband matching between the detector and the antenna, while the stubs tune the resonance of the system at 868 and 2450 MHz. For any operating frequency and incoming RF power, focusing on typical wake-up scenarios ($-60 \div -40$ dBm), the nonlinear regime is optimized accounting for the dispersive behavior of the linear subnetwork (antenna and matching networks), available from electromagnetic simulation, and the nonlinear diode model including its package. The harmonic balance (HB)-based optimization is aimed at enhancing the dc output voltage $V_{\rm dc}$. The final performances of the system are summarized in

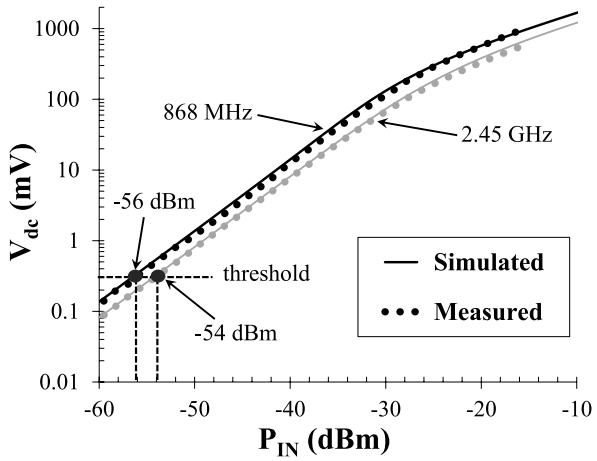

Fig. 3. Simulated and measured WuR detector output voltage versus input power.

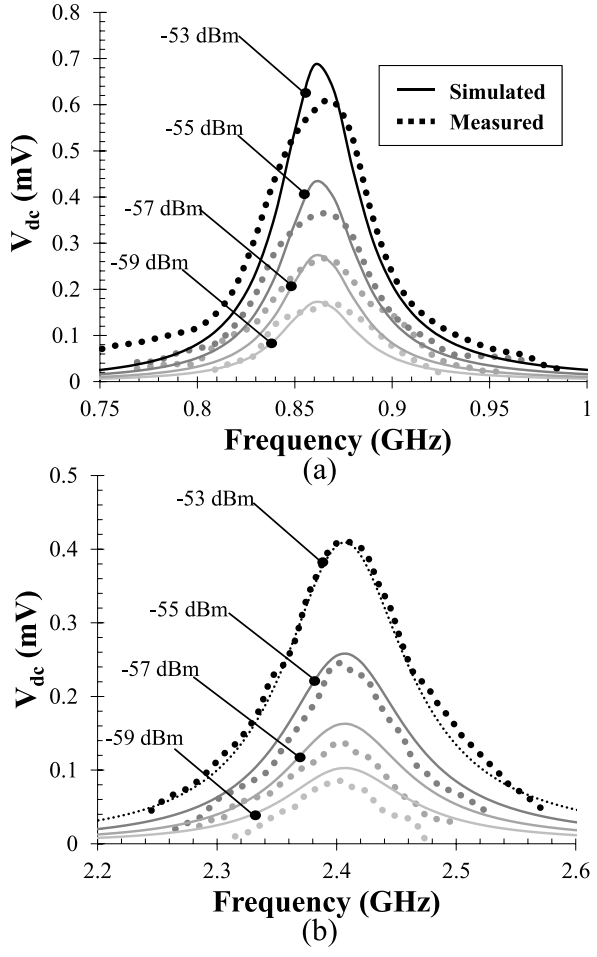

Fig. 4. Predicted and measured dispersive behavior of the detector output voltage for the two operating bands. (a) 868 MHz. (b) 2.45 GHz.

Figs. 3 and 4. Fig. 3 shows the measured and simulated behavior of the output voltage with respect to input power (P_{IN}), for the two operating frequencies, in CW excitation conditions: at -56 dBm the system provides approximately 300 μV at 868 MHz, and to obtain the same dc voltage at 2.45 GHz the required input power is -54 dBm. It is noteworthy that 300 μV is the minimum voltage where the backend comparator is able to detect the incoming signal. As a consequence -56 and -54 dBm can be defined as the system sensitivity for 868 and 2450 MHz bands, respectively. Thus, a 2-dB sensitivity reduction at the higher frequency is observed. This can be explained by considering two effects: 1) the lower diode sensitivity at higher frequencies and 2) the increase in losses of the matching network at 2.45 GHz. Nonetheless, good sensitivity is obtained, compared to the state of the art [11].

Fig. 4 shows the effect of frequency variations on the dc voltage, for the two operating bands and for different power levels. Good agreement between simulations and measurements is again obtained. A slight frequency-shift is observed between the measured and simulated results, the highest measured performances in the two bands being at 860 MHz and 2.41 GHz, respectively.

The baseband WuR subsystem building blocks are: 1) the ultralow power comparator, which generates the demodulated information by detecting the (ultralow) variations at its differential input; 2) the filter; and 3) the microcontroller for the main radio activation. To accomplish the comparator conversion and to overcome the noise effects, an adaptive low power threshold mechanism for the reference pin of the comparator is adopted, which is based on a simple passive bandpass (*RC*) filter on the "$-$" pin of the comparator, while the output is directly connected to the "+" pin. Due to the filter, the comparator can detect the bit '1' by exploiting the differences in the incoming received powers, since the reference signals are based on the received signal level itself. Thus, an important parameter of the comparator is the voltage offset (minimal difference between V+ and V$-$) that determines the minimum sensitivity of the received message.

The adaptive mechanism is designed based on the output signal directly connected to the "+". The backend building blocks in the baseband are: the LPV7215 comparator from Texas Instruments, having an extremely low voltage offset of 300 μV and consuming only 600 nA; the PIC12LF microcontroller from Microchip with only 40 nW at 2 V, in sleep mode, and a fast wake-up time of only 250 μs at 1 MHz. The PIC enables the WuR to match the address by reading the wake-up message.

The baseband WuR subsystem is realized on a low-cost FR4 substrate and its size is 30×40 mm^2. The frontend part dimension of the WuR is 62.5×51 mm^2. The overall dimension of the system is 102.5×63 mm^2, which is compatible with WSN module's dimensions, but can be significantly reduced by merging the RF and baseband sections, including the antenna, in a unique substrate.

III. Optimization of the WuR Excitation Signal

The idea of boosting the operating region of RF/microwave detectors and rectifiers, with optimized non-CW excitations (OW), has been the subject of a large number of studies and experiments [3]–[6], [12], [13]. Indeed non-CW excitations, such as those composed of multisine waveforms, closely spaced in frequency, with high PAPR, enable diodes turn-ON in subintervals of their period, where the CW waves, with the same average power, cannot. It is noteworthy that

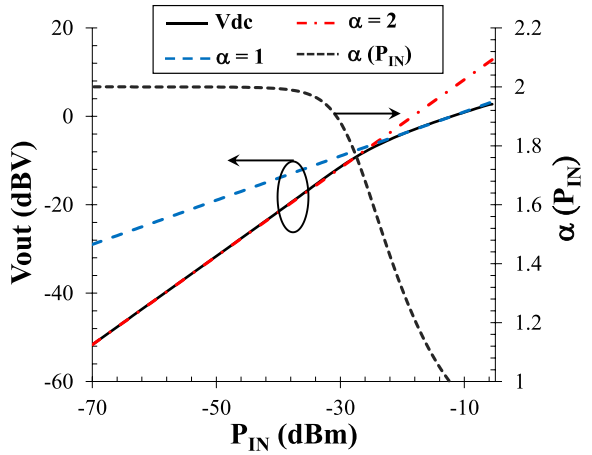

Fig. 5. Simulated behavior of the detector output voltage over the wide power range of interest, and corresponding behavior of the exponential α ($P_{\rm IN}$): for power values from −70 to −35 dBm a quadratic low is confirmed, then it starts decreasing and reaches the 1 value at about −12 dBm. The carrier frequency is 868 MHz.

this situation occurs in a precise range of average input power, depending on the specific diode adopted [3], [12]. The lowest power limit is that enabling the diode turn-ON, and the highest power limit is fixed by the decrease in the maximum efficiency, due to the diode being driven in the breakdown region [6], [8].

This has been proved for RF input power ranging from −30 up to −10 dBm approximately, if using rectifier Schottky diodes such as SMS7630 and HSMS-285B. It has to be noticed that, for EH purposes, the main goal of the detector design is to achieve the highest RF-to-dc efficiency, as well as the minimum dc power and voltage sufficient to bias the rectifier load (consisting of either a sensor or a dc–dc converter) [14], [15]. For this purpose, the load is optimized, together with the rest of the entire system, by nonlinear circuit techniques, for the expected power range of interest [16].

Conversely, for WuR applications the detector load is fixed and it is usually very high (of the order of a few MΩ), being the comparator input impedance. Moreover, the WuR source is a simple modulated signal, usually adopting OOK modulation, which represents data with the presence or absence of the carrier. In this case, the main goal is to achieve the maximum detectable dc voltage, to correctly trigger the ultralow-power comparator [17] rather than the highest conversion efficiency.

In this section, we show that a more convenient choice of the excitation waveform is to exploit duty-cycle reduction of the OOK modulated signal, while ensuring the same average power over the bit period (T_B). In this way, high peaks can be exploited all over the ON interval ($T_{\rm ON}$) of T_B. Obviously the lower the duty cycle and the higher the input peak amplitude, the higher the dc-voltage output. As WuRs operate at low-data rate (typically 1–10 kb/s), highly reduced duty cycles can be exploited without breaching the band limitations regulation.

To select the optimum excitation for the WuR, the RF frontend described in the previous section is first analyzed in CW conditions, for a wide range of (low) input power, spanning from 0 dBm down to −70 dBm by means of HB analysis. The simulated dc-voltage output $V_{\rm dc}$ with respect to the input power P_{IN} is plotted in Fig. 5 in logarithmic scale. The curve is well described by a piecewise linear function [18], satisfying the closed-form relationship

$$V_{\rm dc}(P_{\rm IN}) = V_{d0}(P_{\rm IN}) \cdot \left[\sqrt[2]{P_{\rm IN}}\right]^{\alpha(P_{IN})} \tag{1}$$

which in logarithmic form becomes

$$V_{\rm dc}(P_{\rm IN})|_{dBV} = 10\cdot\log_{10}[V_{d0}P_{\rm IN}] + \frac{\alpha(P_{\rm IN})}{2}\cdot 10\cdot\log_{10}[P_{\rm IN}] \tag{2}$$

where V_{d0} (in dBV) is the intercept of the line at $P_{\rm IN}$ = 0 dBm, while $\alpha(P_{\rm IN})/2$ is its angular coefficient. Three different regions for the linear approximation can be distinguished: 1) the lower power interval ($\alpha = 2$); 2) the higher power interval ($\alpha = 1$); and 3) a transition zone between the two of them. For the present topology, the intercepts at $P_{\rm IN} = 0$ dBm are 4 and 68 for $\alpha = 2$ and $\alpha = 1$, respectively [18].

A suitable figure of merit, to be maximized for the optimum WuR excitation, is the ratio between the dc-voltage envelopes of the OW and of the CW excitations

$$G_V(P_{\rm IN}) = \frac{V_{\rm dc|OW}(P_{\rm IN})}{V_{\rm dc|OW}(P_{\rm IN})} \tag{3}$$

that can be called voltage gain, and it is again a nonlinear function of $P_{\rm IN}$ through (1) as will be shown in Fig. 7. $P_{\rm IN}$ can be rigorously computed as the power received by the antenna by means of the equivalent Thevenin or Norton circuit representation presented in [16]. If the Thevenin equivalent is chosen, the CW voltage generator can be expressed as $V_{\rm CW}(t) = V_{A0}\cos(\omega_0 t)$, and for the optimized waveforms as $V_{\rm OW}(t) = V_A(t)\cos(\omega_0 t)$, where ω_0 represents the carrier angular frequency and $V_A(t)$ represents the low-rate modulated law. For this paper, we assume that the antenna is matched to the rectifier and that its impedance is purely real (R_A). Two families of excitations are considered.

1) Multisine, generated by combining equally and closely spaced N-subcarriers. It can be observed that, for a fixed tone-spacing, peaks increase with the number of tones [5] and the bandwidth as well, while the signal period is fixed.
2) Intermittent excitations carrying the OOK WuR data, generated as square pulses modulating the RF carrier, and intermittently switched ON and OFF with different ON intervals ($T_{\rm ON}$), within the bit period (T_B), to dynamically modify the duty cycle.

To compare the detector performance G_V in terms of its highest output dc voltage at the lowest average power in a bit interval, all the waveforms are designed for the same average power P_B over the bit period T_B, that is, the same energy per bit, and G_V is evaluated with respect to the same time interval, the ON bit period ($T_{\rm ON}$), which is usually much longer than the multisine one.

Fig. 6(a) shows the time behavior of a set of multisine excitations, equally spaced, consisting of N-subcarriers with frequency shift Δf = 500 kHz and 0°-phase shifting among the carriers, as suggested in [5] for EH purposes; tests are carried out using 2, 4, and 8 tones.

For the present case, the signal period $T_{\rm OW}$ is equal to 2 μs. For the ICW excitations a 1-kb data rate is used, corresponding

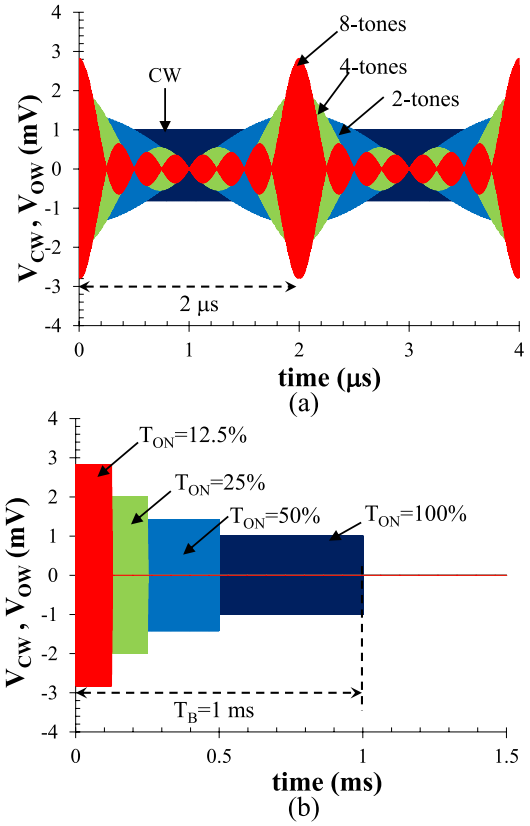

Fig. 6. (a) Multisine waveforms with different number of tones, 500-kHz spaced, with a period of 2 μs [7] and (b) ICW excitations with different "ON" intervals. To compute these excitations an average power per bit of -50 dBm and a WuR bit rate of 1 kHz are used.

to $T_B = 1$ ms. T_{ON} intervals reduced to 50% (500 μs), 25% (250 μs), and 12.5% (125 μs) of T_B are generated. Fig. 6(b) compares the corresponding modulated waveforms, within the same bit interval T_B. To account for the worst case in terms of bandwidth increase, due to the reduced duty cycle, a periodic sequence of "1" and "0" bits is used.

The analytical evaluation of G_V can be obtained by computing the average dc output detector voltage in the same time interval T_{ON} as a function of the CW and of the OW excitations using (3). The following expressions are obtained:

$$V_{dc|OW} = \frac{1}{T_{ON}} \cdot \int_0^{T_{ON}} \left[V_{d0}(P_{IN}) \cdot \sqrt{\frac{V_A^{\alpha(P_{IN})}}{8R_A}} \right] dt \quad (4)$$

$$V_{dc|OW} = \frac{1}{T_{ON}} \cdot \int_0^{T_{ON}} \left[V_{d0}(P_{IN}) \cdot \sqrt{\frac{V_A(t)^{\alpha(P_{IN})}}{8R_A}} \right] dt. \quad (5)$$

For power levels belonging to the diode region where $\alpha = 2$ (see Fig. 5), it is not possible to increase G_V if adopting excitation waveforms having the same average power of the CW counterparts, while this is true when α decreases, as in the second region in Fig. 5. In the latter region, higher values of G_V are obtained by enhancing the peaks in the ON interval (T_{ON}) of T_B, while ensuring the same average power over T_B. This phenomenon is explained by observing that, under intermitted signal excitations, the voltage envelope is forced to its

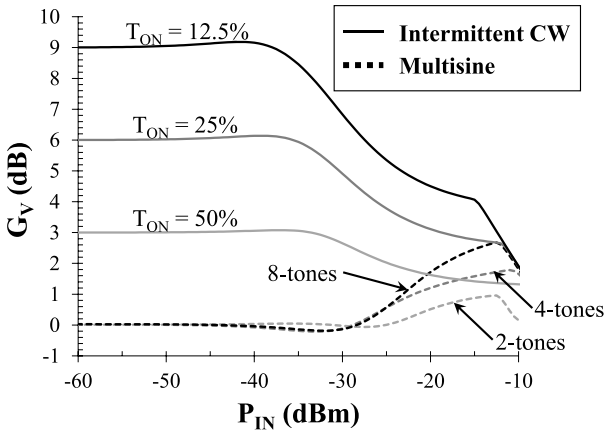

Fig. 7. Simulated results of the voltage gain G_V using multisine and ICW detector excitations, as a function of the average power in a bit interval, which is for the same energy per bit.

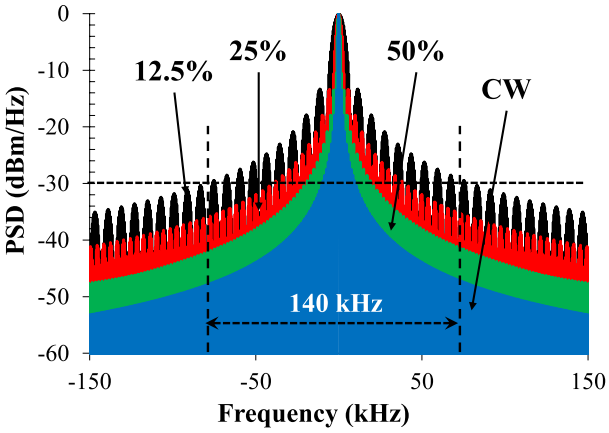

Fig. 8. Simulated spectra of a periodic sequence of 1 and 0 b with a bit period (T_B) of 1 ms and for different T_{ON}.

highest value for a longer time interval than under multisine excitations. This is confirmed by the simulated G_V of the detector excited by the two families of signals discussed above and loaded by the equivalent comparator impedance (1 MΩ). This is shown in Fig. 7, where G_V is plotted in logarithmic scale. The envelope transient HB simulation technique [19] is used to derive these results. These plots show that, for the entire power interval to be exploited for enhancing the WuR sensitivity, higher values of G_V can only be obtained by enhancing the peaks in the ON interval (T_{ON}) of T_B, while ensuring the same average power over T_B. Fig. 7 shows that G_V further increases to 6 and 9 dB if the duty cycle is reduced to 25% and 12.5%, respectively. These results are experimentally confirmed in the next two sections by a lab-level experimental setup and a more realistic setup based on off-the-shelf components.

It is worth noting that in order to fully exploit the POW approach, the control of the POW spectrum is needed to comply with the available regulations. For example, in the RFID UHF band, a 500-kHz channel bandwidth is allowed by the FCC standard [20], and it is reduced to only 200-kHz by (ETSI) [21]. This aspect is considered in Fig. 8 where the simulated spectra for the considered reduced duty cycles are shown. In this figure, it can be observed that in the worst case

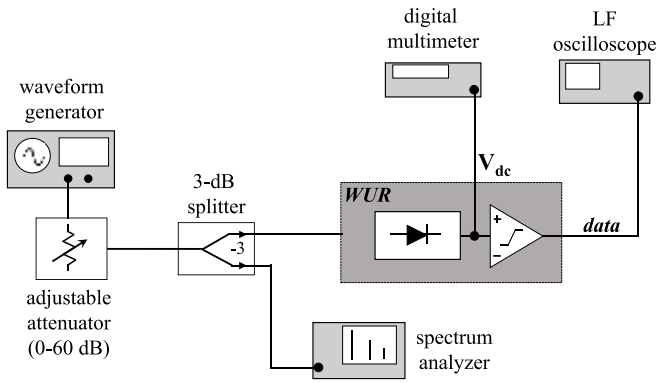

Fig. 9. Block representation of the experimental setup [7].

($T_{ON} = 12.5\%$), the occupied bandwidth is only 140 kHz. This confirms that ICW fully complies with the standards when a low bit rate is involved.

IV. Dual-Band WuR Experimental Results

This section is dedicated to the dual-band experimental validation of the WuR using the ICW excitations that have been demonstrated to be the proper signals able to enhance the WuR sensitivity at the lowest power intervals. As a reference, an average RF power as low as −56 dBm is targeted.

A. Laboratory Setup

Due to the low voltage and power of the signals involved in the POW measurements, special attention has been given to the experimental setup. The adopted setup is schematically depicted in Fig. 9. To generate the designed optimized waveforms, the wideband arbitrary waveform generator Tektronix AWG7122C is used. These optimized signals have been first implemented in MATLAB and then loaded in the generator. The generator output is then connected to a 0.25-dB step digital attenuator (Minicircuit RUDAT-6000) in order to scale the average RF power of the waveforms and keep the same value over a bit interval while reducing the duty cycle. In order to double check such power values, the generator output signal is split in two ways: the first way is used to feed the RF section of the WuR and the second one is connected to a spectrum analyzer (Agilent N1996A), to measure the current average power in any attenuator state. This average power has been measured within a limited bandwidth in order to minimize the noise floor. In fact, to correctly measure the power levels as low as −70 dBm, the spectrum analyzer must be configured in a way that its noise floor does not affect the actual signal. For this scope, the allowed bandwidth has been reduced to 500 kHz and the preamplifier function of the spectrum analyzer is turned ON. With this setup, the noise floor drops to −80 dBm/Hz. Furthermore, to precisely characterize the sensitivity, the detector is directly fed by the waveform generator through the testing port (see Fig. 1) and the antenna is disconnected.

Another critical aspect is the voltage multimeter accuracy in order to precisely measure the detector output dc voltage (V_{dc}), as values as low as 100 μV need to be distinguished. For this purpose, a high-sensitivity digital multimeter (Keithley 2015-THD) with an accuracy of 0.1 μV and typical RMS noise floor of 22 μV is used. However, during the tests a higher noise level of 50 μV has been verified.

Finally, a low-frequency oscilloscope (Agilent DSO X-3024) is used to monitor the comparator activation, as well as the correct reading of the digital data. In this case, the output voltage can be either the comparator bias (V_{DD}) or 0 V. Each measurement procedure is carried out in two steps: in the first step, the averaged power is set (P_{AVG}) and verified by the spectrum analyzer; in the second, the comparator output voltage is measured during the ON-state of the waveforms, when the signal peaks occur. For any waveform under test, the average RF power is spanned from −68 to −15 dBm, with a 0.5-dB step. The maximum power is limited by the maximum voltage swing of the generator. In fact, the waveforms are generated using a range between −1 and 1 V. With this bound, when higher peaks signals (as the PAPRs) are used, the maximum available power decreases.

The WuR is tested under intermittent excitations that are generated as square pulses, modulating the RF carrier, and are intermittently switched ON and OFF with different timings, within the bit interval, to dynamically modify the duty cycle. For the present experiment, square pulses with 50%, 25%, and 12.5% duty cycles are considered. For the bit interval, we adopt the same symbol rate of 1 kb/s ($T_B = 1$ ms) for any ICWs, which is typical of WuR operation. With such a low bit rate, for any optimized wake-up signal, no pulse shaping is performed to control the signal bandwidth. For the sake of simplicity, the performances are measured using a sequence of "1" and "0" bits, continuously repeated.

B. Results and Discussion

Figs. 10 and 11 show the results for the intermittent signals, versus the average RF power. Fig. 10 shows the dc output voltage resulting from different duty cycles at 868 MHz [Fig. 10(a)] and 2.45 GHz [Fig. 10(b)]. These plots demonstrate that, by decreasing the duty cycle, the detector output voltage increases and this is especially true at the lowest power levels. In particular, for the 868-MHz case, the system sensitivity is approximately −56 dBm in CW conditions ($T_{ON} = 100\%$), while it improves down to −65 dBm with $T_{ON} = 12.5\%$. Similar results can be observed at the second WuR operating frequency of 2.45 GHz: in CW conditions ($T_{ON} = 100\%$) the sensitivity is −54 dBm, while it goes down to −63 dBm with a $T_{ON} = 12.5\%$. The measured results of the detector figure of merit Gv, which is defined in Section III, are plotted in Fig. 11(a) and (b) for carriers at 868 MHz and 2.45 GHz, respectively, and are compared with the predicted ones: the chosen excitation waveforms demonstrate that an increase of Gv can be obtained over a large range of ultralow power values, starting from −65 dBm, or −63 dBm, depending on the carrier frequency.

For any chosen "ON" interval (T_{ON}), the gain is almost constant and starts decreasing at the levels where the diode saturation is explored. Fig. 11(a) and (b) shows that reducing T_{ON} results in an increase in the gain for lower power levels, due to increase in the excitation peaks. In addition, Fig. 11 shows that a 3-dB gain with $T_{ON} = 50\%$ is obtained approximately, and

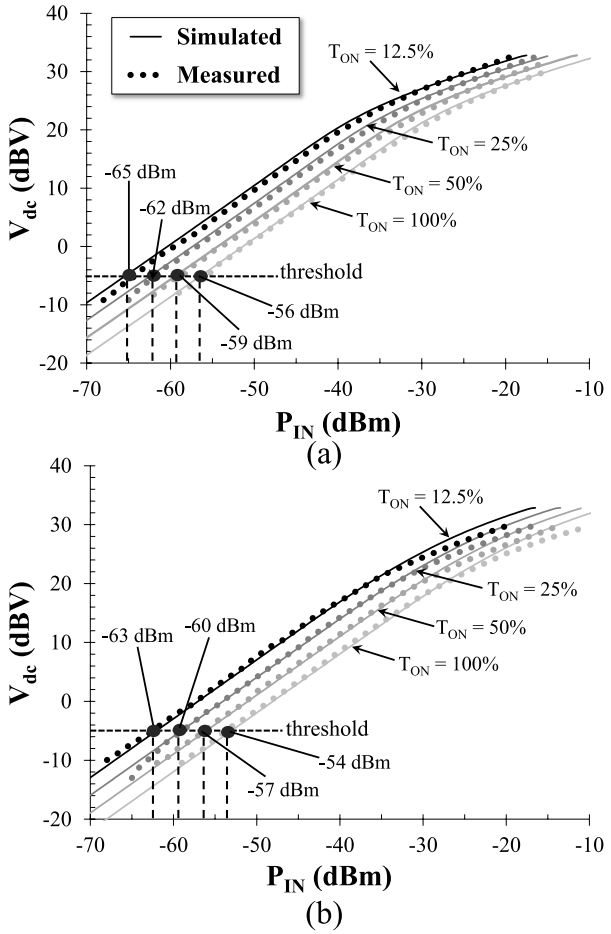

Fig. 10. Dual-band measured and predicted performance of the RF subsystem, in terms of detector output voltage, as a function of the average power in a bit interval, which is for the same energy per bit for a carrier frequency of (a) 868 MHz and (b) 2.45 GHz.

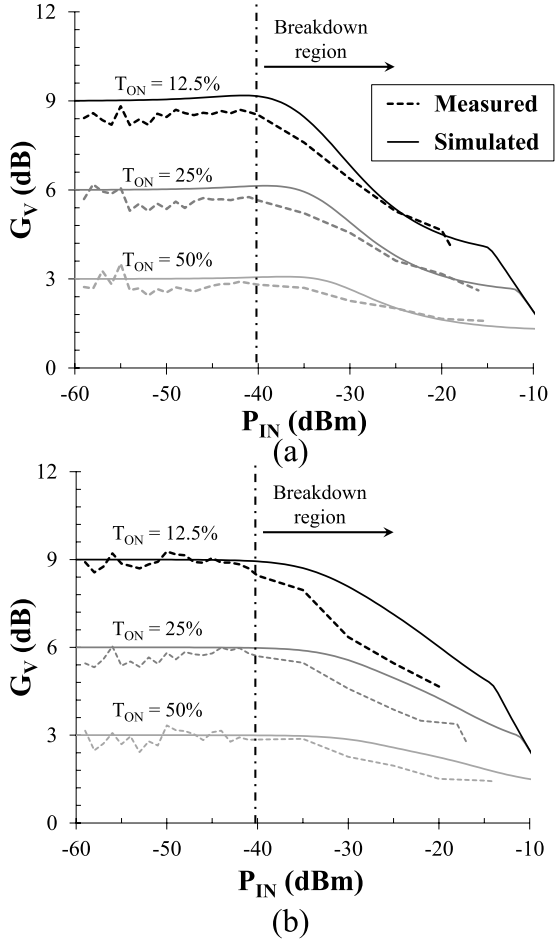

Fig. 11. Dual-band measured and predicted results in terms of obtainable detector voltage gain for the selected WuR excitation waveforms, as a function of the average power in a bit interval, which is for the same energy per bit for a carrier frequency of (a) 868 MHz and (b) 2.45 GHz.

increases to 6 and 9 dB if T_{ON} is reduced to 25% and 12.5%, respectively. Very good agreement of the measured behavior is observed with respect to the predicted ones.

C. WuR Excitations Implemented by Off-the-Shelf Components

In this section, we show that the proposed WuR excitation strategy, which was experimentally validated using lab-level instrumentations, can be fully implemented using commercial off-the-shelf components to generate the optimized WuR excitations. The developed test bed is shown in Fig. 12: it consists of a demo board from TI, using the transmitter (EM430-F6137RF900), an attenuator, and the described WuR as receiver; the attenuator is used to emulate the free space path loss. The TI transmitter hosts a microcontroller with integrated radio (TI CC430F6137). Due to the considered transmitter, only the 868-MHz band is considered. The other WuR operating band (2.45 GHz) can be tested as well, with a different proper transmitter, without loss of generality. The chosen setup allows to dynamically control all the parameters of interest for the purpose of this demonstration, such as data rate, transmitted power, and bit sequence to be sent.

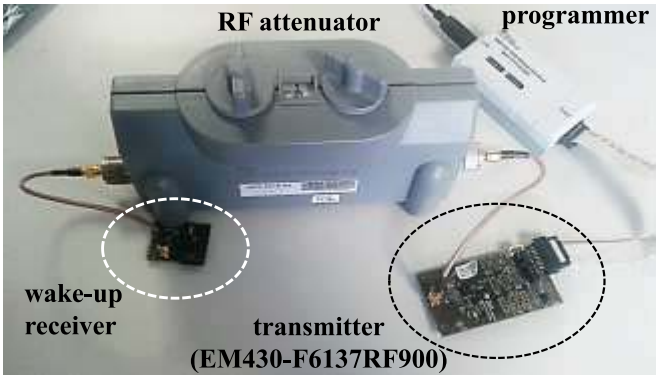

Fig. 12. Block representation of the experimental setup.

Specifically, four different configurations have been set according to the T_{ON} intervals considered for testing the WuR. The bit period used for these analyses was 10 ms (0.1 kHz). Thus, such configurations can be categorized by the ON period and the transmitter output power P_{OUT}, which is adjusted according to T_{ON} changes, in order to keep the same average power for any configuration. Specifically for the measurement conditions where: 1) $T_{ON} = 10$ ms, $P_{OUT} = 0$ dBm; 2) $T_{ON} = 5$ ms (0.2 kHz), $P_{OUT} = 2.5$ dBm; 3) $T_{ON} = 3.33$ ms,

TABLE I
SUMMARY OF THE WUR SENSITIVITY WITH OFF-THE-SHELF COMPONENTS

setup	*a)*	*b)*	*c)*	*d)*
P_{OUT} (dBm)	0	2.5	4.5	10
Bit rate (kbps)	0.1	0.2	0.3	1
Average Input power (dBm)	~ 0	~ 0	~ 0	~ 0
Achieved Sensitivity (dBm)	-56	-57.5	-60.2	-64

$P_{\mathrm{OUT}} = 4.5$ dBm; and 4) $T_{\mathrm{ON}} = 1$ ms, $P_{\mathrm{OUT}} = 10$ dBm, these values have been selected considering the available settings of the demo board. The address message to be detected at the WuR side was "$0 \times$ AA," corresponding to the 8-b sequence "10101010."

For all the configurations under test, the minimum power enabling the correct data reception was registered and the results are summarized in Table I: it is possible to notice that, using the proposed optimized excitations, configuration d) allows a successful data transmission at an average power that is 8 dB lower than that needed by configuration a).

V. CONCLUSION

The dual-band operation of a state-of-the-art passive WuR with enhanced sensitivity has been demonstrated in this paper. The RF section of the WuR consists of a multiband antenna, optimally matched, at the two operating frequency bands, to a diode-based detector that is loaded by an ultralow-power comparator. Such an RF configuration is very similar to a rectenna system designed for EH application. However, in the present design, the main goal is to achieve the maximum detectable dc voltage at the minimum average RF received power, to correctly trigger the ultralow-power baseband section of the WuR, rather than to reach the maximum conversion efficiency. Analytical and experimental studies have been carried out to define the optimum modulated excitations, in order to enable the WuR operations, starting from RF received power as low as -65 dBm. The best solution is derived by taking advantage of the simple modulated law adopted for generating the wake-up signal, based on the absence or presence of the carrier: high peaks in a reduced duty cycle can be generated, while ensuring the same average power over the bit period. This does not cause sampling failure, thanks to the low-data rate (typically 1–10 kb/s) adopted by WuR, nor exceeding the allowed spectrum. The correct addressing of the WuR at such low powers is first verified in a laboratory setup for the proposed sources at the two frequency bands and the correct detection of a precise address has been obtained experimentally using average power lower than -60 dBm, for both the bands. Finally, it has been demonstrated that such optimized excitations can be exploited by commercial transceivers, by suitably configuring their operations, and similar performance have been tested with such configurations.

REFERENCES

[1] M. Magno and L. Benini, "An ultra low power high sensitivity wake-up radio receiver with addressing capability," in *Proc. IEEE 10th Int. Conf. Wireless Mobile Comput. Netw. Commun. (WiMob)*, Oct. 2014, pp. 92–99.

[2] M. Del Prete, D. Masotti, A. Costanzo, M. Magno, and L. Benini, "A 2.4 GHz-868 MHz dual-band wake-up radio for wireless sensor network and IoT," in *Proc. IEEE 11th Int. Conf. Wireless Mobile Comput., Netw. Commun. (WiMob)*, Oct. 2015, pp. 322–328.

[3] M. S. Trotter, J. D. Griffin, and G. D. Durgin, "Power-optimized waveforms for improving the range and reliability of RFID systems," in *Proc. IEEE Int. Conf. RFID*, Apr. 2009, pp. 80–87.

[4] A. J. S. Boaventura and N. Carvalho, "Extending reading range of commercial RFID readers," *IEEE Trans. Microw. Theory Techn.*, vol. 61, no. 1, pp. 633–640, Jan. 2013.

[5] A. Boaventura, D. Belo, R. Fernandes, A. Collado, A. Georgiadis, and N. B. Carvalho, "Boosting the efficiency: Unconventional waveform design for efficient wireless power transfer," *IEEE Microw. Mag.*, vol. 16, no. 3, pp. 87–96, Apr. 2015.

[6] C. R. Valenta, M. M. Morys, and G. D. Durgin, "Theoretical energy-conversion efficiency for energy-harvesting circuits under power-optimized waveform excitation," *IEEE Trans. Microw. Theory Techn.*, vol. 63, no. 5, pp. 1758–1767, May 2015.

[7] M. Del Prete, A. Costanzo, D. Masotti, T. Polonelli, M. Magno, and L. Benini, "Experimental analysis of power optimized waveforms for enhancing wake-up radio sensitivity," in *Proc. IEEE Int. Microw. Symp.*, May 2016, pp. 1–4.

[8] H. Matsumoto and K. Takei, "An experimental study of passive UHF RFID system with longer communication range," in *Proc. Asia–Pacific Microw. Conf.*, Dec. 2007, pp. 1–4.

[9] M. Del Prete, D. Masotti, A. Costanzo, M. Magno, and L. Benini, "A dual-band wake-up radio for ultra-low power wireless sensor networks," in *Proc. IEEE Topical Conf. Wireless Sensors Sensor Netw. (WiSNet)*, Austin, TX, USA, Jan. 2016, pp. 81–84.

[10] A. Costanzo, M. Fabiani, A. Romani, D. Masotti, and V. Rizzoli, "Co-design of ultra-low power RF/Microwave receivers and converters for RFID and energy harvesting applications," in *IEEE MTT-S Int. Microw. Symp. Dig.*, May 2010, pp. 856–859.

[11] V. Jelicic, M. Magno, D. Brunelli, V. Bilas, and L. Benini, "Benefits of wake-up radio in energy-efficient multimodal surveillance wireless sensor network," *IEEE Sensors J.*, vol. 14, no. 9, pp. 3210–3220, Sep. 2014.

[12] C. R. Valenta and G. D. Durgin, "Rectenna performance under power-optimized waveform excitation," in *Proc. IEEE Int. Conf. RFID (RFID)*, Apr. 2013, pp. 237–244.

[13] H. Sakaki, T. Kuwahara, S. Yoshida, S. Kawasaki, and K. Nishikawa, "Analysis of rectifier RF-DC power conversion behavior with QPSK and 16QAM input signals for WiCoPT system," in *Proc. Asia–Pacific Microw. Conf. (APMC)*, Nov. 2014, pp. 603–605.

[14] S. Kim *et al.*, "Ambient RF energy-harvesting technologies for self-sustainable standalone wireless sensor platforms," *Proc. IEEE*, vol. 102, no. 11, pp. 1649–1666, Nov. 2014.

[15] M. Dini *et al.*, "A fully-autonomous integrated RF energy harvesting system for wearable applications," in *Proc. Eur. Microw. Conf. (EuMC)*, Nuremberg, Germany, Oct. 2013, pp. 987–990.

[16] A. Costanzo *et al.*, "Electromagnetic energy harvesting and wireless power transmission: A unified approach," *Proc. IEEE*, vol. 102, no. 11, pp. 1692–1711, Nov. 2014.

[17] M. Magno, V. Jelicic, B. Srbinovski, V. Bilas, E. Popovici, and L. Benini, "Design, implementation, and performance evaluation of a flexible low-latency nanowatt wake-up radio receiver," *IEEE Trans. Ind. Informat.*, vol. 12, no. 2, pp. 633–644, Apr. 2016.

[18] S. Wetenkamp, "Comparison of single diode vs. dual diode detectors for microwave power detection," in *IEEE MTT-S Int. Microw. Symp. Dig.*, Boston, MA, USA, May 1983, pp. 361–363.

[19] V. Rizzoli, D. Masotti, F. Mastri, and E. Montanari, "System-oriented harmonic-balance algorithms for circuit-level simulation," *IEEE Trans. Comput.-Aided Des. Integr. Circuits Syst.*, vol. 30, no. 2, pp. 256–269, Feb. 2011.

[20] "Operation within the bands 902–908 MHz, 2400–2483.5 MHz, and 5725–5850 MHz," FCC, FCC Doc. 47 CFR 15.247, 2014.

[21] "Radio frequency identification equipment operating in the band 865 MHz to 868 MHz with power levels up to 2 W," ETSI, ETSI Doc. EN 302 3208-1 V1.2.1, 2008.

Massimo Del Prete (S'15) received the B.S. and M.S. degrees in telecommunication engineering from the University of Bologna, Bologna, Italy, in 2007 and 2011, respectively, where he is currently pursuing the Ph.D. degree with the Department of Electrical, Electronic, and Information Engineering.

His current research interests include wearable and multiband antennas, CAD of microwave integrated circuits, with a special emphasis on low-power rectenna, power management for autonomous sensors, and wireless power transmission.

Alessandra Costanzo (M'99–SM'13) has been an Associate Professor of electromagnetic fields with the University of Bologna, Bologna, Italy, since 2001. She has coauthored more than 150 scientific publications on peer-reviewed international journals and conferences and three book chapters and holds two European and one U.S. patent. Recently, she has developed innovative wireless power systems for both far- and near-field solutions. Her current research interests include multidomain design (based on nonlinear/electromagnetic co-simulation) of entire wireless links, such as RFID, multi-in multi-out, and UWB, including rigorous modeling of radiating elements and realistic channel models.

Prof. Costanzo is the Chair of the IEEE MTT-26 Technical Committee on Wireless Energy Transfer and Conversion, and an MTT-S Representative of the IEEE Council on RFID. She is an associate editor of the *Cambridge Wireless Power Transfer Journal* and the *International Journal of Microwave and Wireless Technologies*. She is the Chair of WG1: "far-field wireless power transfer.

Michele Magno (SM'13) received the M.S. and Ph.D. degrees in electronic engineering from the University of Bologna, Bologna, Italy, in 2004 and 2010, respectively.

Currently, he is a Post-Doctoral Researcher with ETH Zurich, Zurich, Switzerland, and a Research Fellow with the University of Bologna. He has collaborated with several universities and research centers, such as University College Cork and Tyndall Institute, Cork, Ireland, Imperial College London, London, U.K., the University of Trento, Trento, Italy, the Politecnico di Torino, Turin, Italy, and the University of British Columbia, Vancouver, BC, Canada. He has authored more than 70 papers in international journals and conferences. His current research interests include wireless sensor networks, wearable devices, energy harvesting, low-power management techniques, and extension of lifetime of battery-operated devices.

Diego Masotti (M'00) received the Ph.D. degree in electric engineering from the University of Bologna, Bologna, Italy, in 1997.

In 1998, he joined the University of Bologna as a Research Associate of electromagnetic fields. His current research interests include nonlinear microwave circuit simulation and design, with an emphasis on nonlinear/electromagnetic co-design of integrated radiating subsystems/systems for wireless power transfer and energy harvesting applications.

Dr. Masotti has been on the Editorial Board of the *International Journal of Antennas and Propagation* and has been a member of the Paper Review Board of the IEEE TRANSACTIONS ON MICROWAVE THEORY AND TECHNIQUES since 2004.

Luca Benini (F'07) is a Full Professor with the University of Bologna, Bologna, Italy, and is the Chair of the Digital Circuits and Systems with ETHZ, Zurich, Switzerland. He was the Chief Architect for the Platform2012/STHORM project at STMicroelectronics, Grenoble, France, from 2009 to 2013. He held visiting and consulting researcher positions with EPFL, IMEC, Hewlett-Packard Laboratories, and Stanford University. He has authored more than 700 papers in peer-reviewed international journals and conferences, four books, and several book chapters. His current research interests include energy-efficient system design, multicore SoC design, energy-efficient smart sensors, and sensor networks for biomedical and ambient intelligence applications.

Prof. Benini is a member of the Academia Europaea.